Steam Turbine Last Stage under Low-load Conditions

Michal Hoznedl[1]*, *Tereza* Dadáková[2], *Tereza* Kubíková[3], and *David* Hron[4]

[1]Doosan Škoda Power a.s., Experimental Research, 301 28, Tylova 1/57, Plzeň, Czech Republic
[2]Doosan Škoda Power a.s., Measurement & Diagnostics, 301 28, Tylova 1/57, Plzeň, Czech Republic
[3]University of West Bohemia, Power system engineering department, 301 00, Univerzitní 8, Plzeň, Czech Republic
[4]Doosan Škoda Power a.s., Thermodynamics, 32300, Tylova 1/57, Plzeň, Czech Republic

Abstract. The low and variable load regimes of steam turbines have become a highly topical issue in recent times. Steam turbines frequently balance fluctuations in the power grid or operate with a heat source that has variable parameters, such as waste incineration plants. In such cases, the steam can have wetness content locally up to 19 %. During operation with variable output, compression, heating, and the formation of vibrations occur in the tips of the last stage rotating blades. Steam flows only through a portion of the available cross-section, while the remainder flows in reverse. Under such conditions, it is necessary to cool the exhaust section of the turbine. This paper describes contemporary knowledge regarding the behaviour of the steam flow and tip vibrations of rotating blades across various operating regimes. The flow parameters are monitored using pneumatic probes and local pressure and temperature measurements, while the vibration amplitudes are measured using the blade tip-timing method.

1 Introduction

Steam turbines are currently operated not only at nominal power but across a wide range of regimes. During turbine operation, the inlet pressure and steam temperature to the turbine often change over time, which also affects the flow rate. Some turbines have significant steam extraction during expansion for subsequent technology. The amount of steam drawn can also change over time based on process demands. The pressure at the turbine outlet is often unstable, varying significantly, particularly when using air-cooled condensers. More time-stable water cooling is not commonly used for smaller machines.

Especially low operating regimes of steam turbines, where the power over an extended period is lower than 20% of the nominal power, pose several risks to the machine. In low-load regimes, the phenomena described below occur mainly in the area of the last stages and the exhaust hood.

The amount of steam is too small to fill the entire flow cross-section of the last stage. The steam is centrifuged by the last rotor blade towards the outer casing wall [1]. The steam then flows from the last stage into the exhaust hood only near the outer periphery. However, often

* Corresponding author: michal.hoznedl@doosan.com

the steam does not fill the space around the entire periphery and flows only through parts of the periphery, forming certain bands. The schematic representation of steam flow at low mode is shown in Fig. 1.

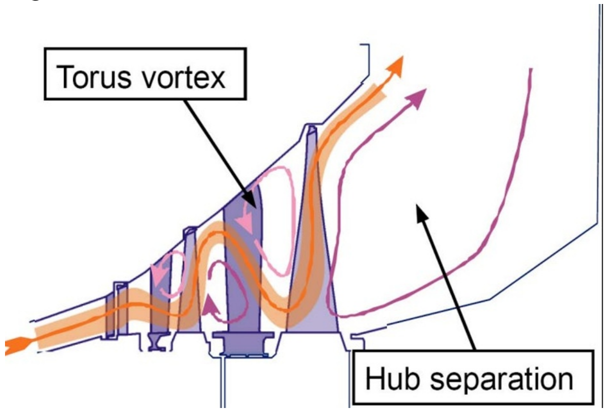

Fig. 1. Meridional flow field under low-load conditions.

Such flow is inherently unsteady [2, 3]. The axial exit velocity from the last blade is low, often leading to steam being drawn from the outlet region back into the last stage [4]. Conversely, at the blade tip, the velocity vector is at Ma = 1, resulting in a substantial rotational component of the exit velocity c_{2u}, and the steam exit angle α_2 near the blade tip approaches 160°. This assumes that in the case of axial exit, $\alpha_2 = 90°$.

The radial movement of the steam is enabled because the last rotor blade, or multiple rows of blades, behaves like a centrifugal compressor. As a result, especially the last stage or multiple stages consume work. The work is primarily generated by the first stages of the turbine. However, the total power generated by the turbine is low, often below 10% of the nominal power. The pressure ratio across the blade tip $\pi = p_{2t} / p_{1t}$ is higher than 1 in such cases [1]. The schematic behavior of the pressure ratio relative to the axial exit velocity is shown in Fig. 2.

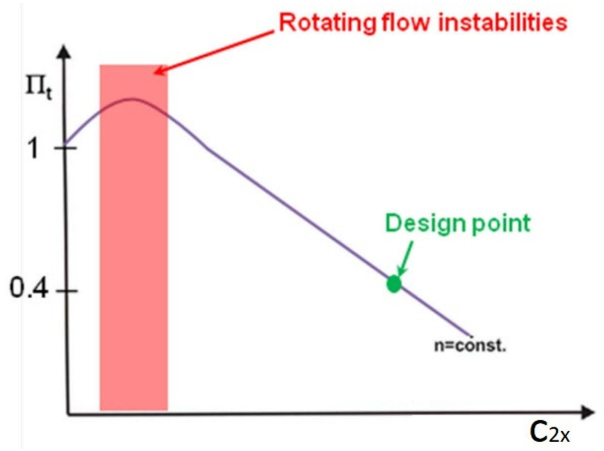

Fig. 2. Pressure ratio over last rotor blade tip.

Similar statements hold for the temperature ratio $\tau = t_{2t} / t_{1t}$. Consequently, there is significant heating of the exhaust steam [5]. High-temperature steam poses a risk to downstream equipment (heat exchangers, air-cooled condensers), where overheating may occur. There may also be issues with local heating of the root section behind the last stage, the location of the bearing. Localized heating can lead to vibrations in the turbine and its shutdown.

Therefore, during low-load regimes, it is necessary to cool the steam turbine exhaust using water nozzles, typically supplied from the discharge of condensate pumps. The amount and angle of the cooling water jet must be such that erosion of the trailing edges of the rotor blades at the root is avoided, see the purple trajectory in Fig. 1. Certain limits of these methods are covered by numerical [6, 7] and very rarely experimental [8] research. Nevertheless, the danger of trailing edge erosion at the root is significant. The close-to-root profiles are critical from the perspective of mechanical stress. An example of real and numerically identified erosion on the trailing edges of rotor blades [6] is shown in Fig. 3.

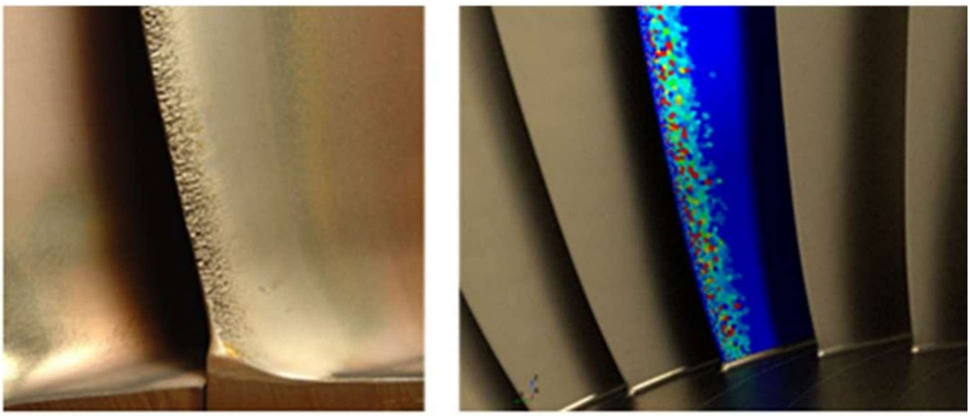

Fig. 3. Field service photograph and numerically obtained erosion.

During low-load regimes, the turbine's steam flow is unsteady. There is a separation of the flow from the wetted profiles. This causes vibrations at the tips of the last blades, which need to be damped using mechanical connections, known as tie-bosses [9].

It is evident that all described phenomena need to be experimentally tested. Numerous measurements have been carried out on model turbines or numerically. Experiments on real-size turbines do not exist or have not yet been published. The presented article aims to supplement the information about the behavior of a turbine operating across a wide range of regimes.

2 Turbine and measurement description

Experiments were conducted on a steam turbine with a maximum power output of 210 MW, featuring an axial exhaust into an air-cooled condenser. The basic parameters of the turbine and the last stage are provided in Table 1:

Table 1. Steam turbine basic parameters.

Parameter	Value	Unit
Rotational speed n	3600	rpm
Last stage blade root diameter D_p	1416	mm
Last stage blade length L	729	mm
Number of last stage nozzles n_N	48	-

Number of last stage buckets n_B	50	-
Last stage inlet pressure p_0	0.25106	bar
Last stage outlet pressure p_2	0.11376	bar
Ventilation below φ_z	0.181	-

In the area of the last stage and the exhaust hood, a total of 24 wall taps for static pressure measurements "p," 22 temperature measurements of the steam flow "t," and ports for pneumatic probe “s before and after the last stage of the turbine, as well as at the outlet of the axial casing, were installed. The static pressure taps and thermometers were placed at a minimal distance from each other to reduce measurement error when determining steam parameters at the given locations. The meridional section of the turbine and the positions of the measurement points are shown in Fig. 4. All measurement points were duplicated and located on both sides of the turbine, 15 to 20° above the horizontal joint. For further analysis, the relevant pressures and temperatures are in planes 1 and 2, that is, before and after the rotor blade and at the root "r" and the tip "t."

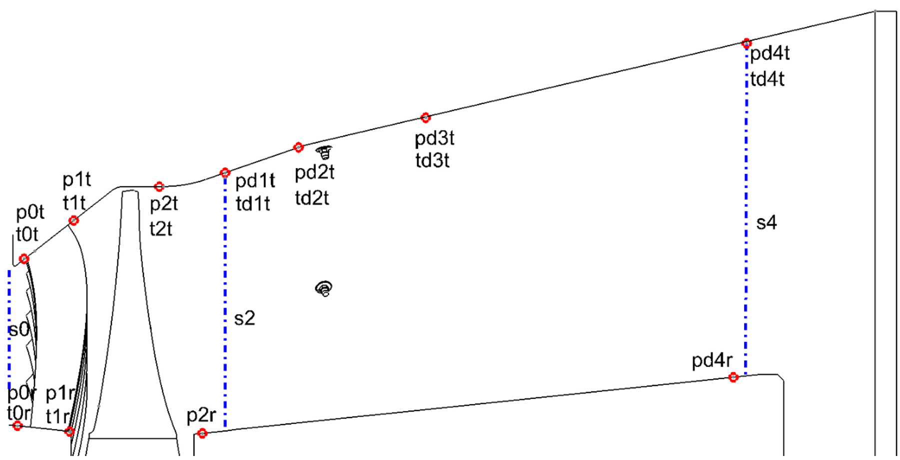

Fig. 4. Turbine cross-section with positions of measuring places.

Impulse pipings were blown automatically about every 10 minutes for 5 seconds by atmospheric air to clean them from condensed water droplets. Measurement of static pressures using static pressure taps and probes was carried out using pressure scanners NetScanner 9022 and sensors NetScanner 9401 with the range of 0-1 bar. The combined standard uncertainty of measurement of the static pressure at the level 2σ for the condenser pressure 5000 Pa is ± 110 Pa. Real uncertainty seems to be lower, around ± 40 Pa.

Temperatures were measured using flexible resistance thermometers Pt100 with accuracy class A by using of NI cDAQ. Uncertainty of temperature measurement was ±0.4 °C.

For flow field probing the 7-hole disc probe was used with the stem diameter of 30 mm, and with the head disc diameter of 20 mm. Four pressure taps were installed along the disk periphery in order to define the meridial angle of the steam flow. Two more taps were used to balance the probe in the flow and the last pressure tap on the side of the probe was used to define the static pressure. Turning the probe in the circumferential direction made it possible to define angle α in any direction The traversing step was chosen to be 25 mm. The probe positions are schematically shown by dashed lines in Fig. 4. The measurement uncertainty of the probe radial position is ± 0.5 mm and aerodynamic probe sensitivity to angle α is ± 0.5°.

All seven pressure pipes were continuously blown by atmospheric air. This reduced the possibility of pressure pipes being clogged by water droplets. The blow causes a systematic measurement error that is the same on all pressure pipes and is at the level of 10 Pa.

The blade vibrations were measured with Blade Tip-Timing using in house made eddy-current sensors and acquisition HW from HoodTech Corporation based on NI solution. It was necessary to process the data using the special software which can work with under-sampled data and multiple non-equidistant space sensors. For this measurement the 8 eddy-current sensors were installed in group of 5 and 3. The larger group was located on the trailing edge and the second one on the leading edge. These two axial positions above the blade shroud were selected to provide more accurate amplitude in terms of sensor blade calibration.

The in-house developed acquisition software provides accurate amplitude of all nodal diameters for each of monitored blades. The blades are monitored during multiple operation regimes (different blade loading caused by backpressure or steam mass flow).

3 Results

The operation characteristics of the turbine can be defined with respect to the behavior of the last stage and its transition to ventilation using the so-called ventilation coefficient φ:

$$\varphi = c_{2x} / u \tag{1}$$

Here, c_{2x} is the axial exit velocity from the last stage, calculated using Stodola's cone based on pressure measurements in the condenser and the nearest higher measured pressure. The value u is the peripheral velocity at the mean diameter of the rotor blade. In the case of the measured turbine, u = 404.3 m/s. The transition to ventilation occurs when the limit value $\varphi = \varphi_z = 0.181$. If $\varphi < \varphi_z$, then the last stage is in the ventilation, low-load, regime.

The first evaluated parameter is the pressure recovery factor c_{p4} between the exit from the rotor blade and gradually at the root "r" and the tip "t" at the casing exit. The pressure recovery factor serves to estimate the quality of the exhaust hood. The higher its value, the better the exhaust hood compresses the steam at the blade exit, thus extending the turbine's expansion line. The pressure recovery for the root and tip sections of the casing are defined as:

$$c_{p4r} = (p_{4r} - p_2) / p_{dyn2} \tag{2}$$
$$c_{p4t} = (p_{4t} - p_2) / p_{dyn2} \tag{3}$$

The maximum values of φ indicate that the last stage is overloaded, and the exit velocity is high. Therefore, the stage does not operate at the economic optimum despite the high pressure recovery. The economic optimum lies in the interval $0.35 < \varphi < 0.60$.

A detailed view of the static pressure profile along the length of the outer casing wall for one side is shown in Fig. 6. Here, the pressure p_x is progressively expressed as p_{d1t}, p_{d2t}, p_{d3t}, and p_{d4t}, from which the pressure behind the blade tip p_2 is subtracted for each measurement. For ventilation regimes, it is clear that the flow is unstable, and the pressures are roughly the same, except for the section between p_{d3t} and p_{d4t}, where some compression occurs. For nominal and overloaded behavior of the last stage, the highest compression is in the region of p_{d2t} and p_{d3t}. Compression increases with the exit velocity, but between p_{d3t} and p_{d4t}, it is negligible. In the area of aerodynamic choking at the exit of the last stage, shock waves form in the casing, see Fig. 5 at the bottom right, leading to a significant drop in all pressures, especially p_{d1t} and p_{d2t}, which are close to the shock waves. Consequently, there is a significant pressure loss in the exhaust hood instead of the expected pressure gain.

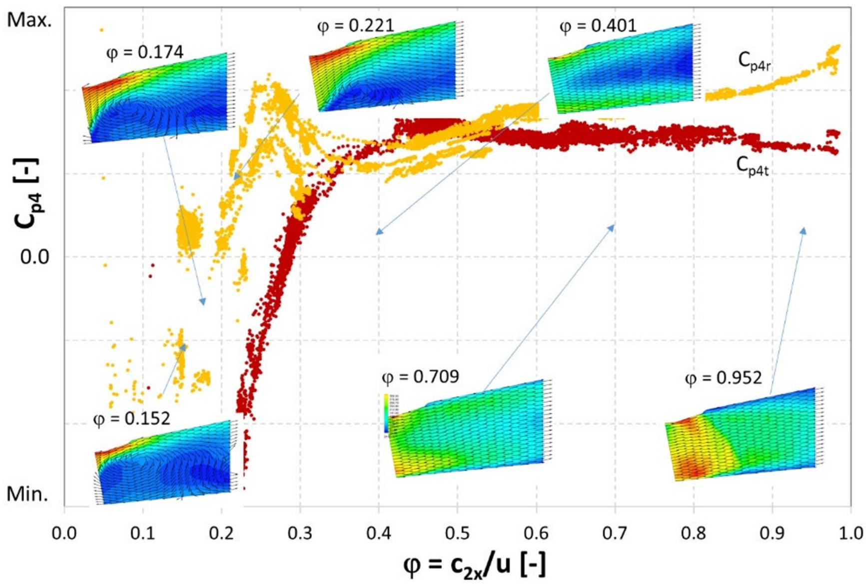

Fig. 5. Pressure recovery for root and tip cross-section.

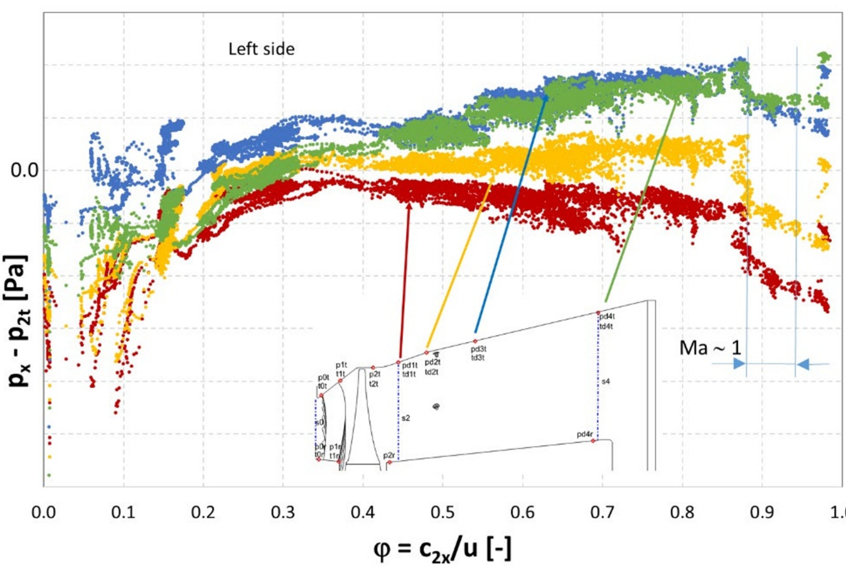

Fig. 6. Pressure increase over the ventilation factor and exhaust hood length – left side.

From the other side, see Fig. 7, the profiles are similar, but the compression is significantly lower. This is due to the rotation of the steam flow and the placement of the pressure taps in the wake regions behind the reinforcing ribs. When evaluating the experiment, it is essential to carefully consider the credibility of the data and compare it with the results of CFD calculations.

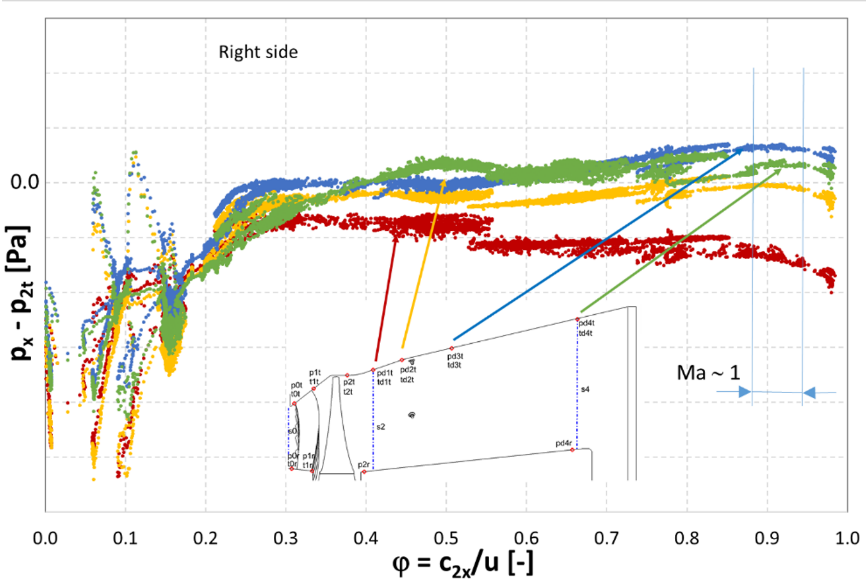

Fig. 7. Pressure increase over the ventilation factor and exhaust hood length – right side.

The behavior of the last stage can be expressed from the knowledge of the mean pressures before the stage p_0 and after the stage p_2. From Fig. 8, it is evident that the points located below the dashed line indicate conditions where compression occurred in the last stage, meaning $p_2 > p_0$. In such cases, of course, $c_{2x} / u \rightarrow 0$.

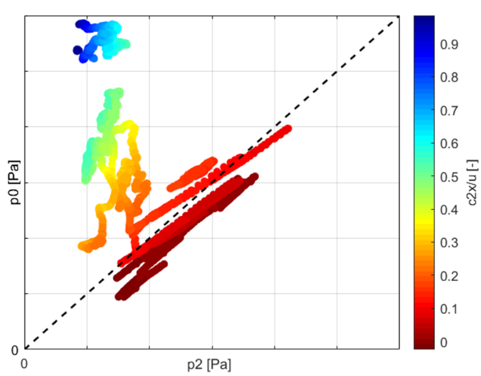

Fig. 8. Pressures around last stage and ventilation coefficient.

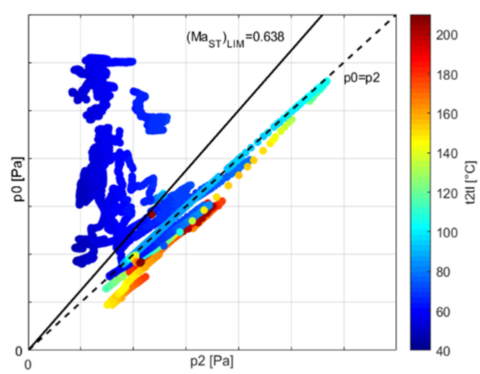

Fig. 9. Pressures around last stage and t_{2tl} temperature.

From the turbine design perspective, it is essential to know under what conditions compressive heating of the steam will occur around the last stage and what the maximum achievable temperature value at point t_{2t} will be. This is shown in Fig. 9. It is evident that the steam at the blade tip heats up to approximately 210 °C, while the saturation temperature for the given pressure is around 60°C. The steam is significantly superheated and theoretically free of water droplets. The limiting Mach number of the stage $(Ma_{ST})_{LIM}$ occurs when $p_{2t} > p_{1t}$. That is, when compression occurs only at the blade tip. In such a case, an isolated increase in temperature t_{2t} begins.

Probing can provide useful data to verify the behavior of the last stage. The distribution of meridional velocity components in planes before the last stage 0, after the last stage 2, and at the casing exit 4 for nominal regime (φ ≅ 0.35) is shown in Fig. 10. The velocity is evenly distributed across all three measured profiles, with no flow disturbances observed. Probing in plane 0 down to the root was not possible for technical reasons.

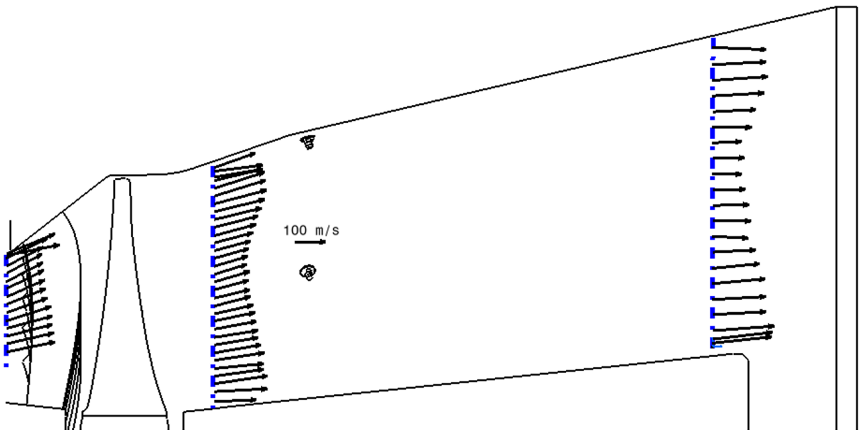

Fig. 10. Measured meridional velocities for nominal regime (φ ≅ 0.35).

The situation is different when the turbine is in ventilation regime. Near the outer exhaust hood wall, the velocity is high, while towards the root, the velocity significantly decreases, and below half the length of the blade, the steam velocity is immeasurably low.

When determining steam velocity using a pneumatic probe, the measured dynamic pressure is the starting point. The uncertainty in its measurement is ±110 Pa. This means that if the measured dynamic steam pressure is lower than 110 Pa, it is subject to high uncertainty. The dynamic steam pressure also depends on the density, which is a function of the static steam pressure and wetness. For wetness y = 0.92, the boundary between reliably measurable and unmeasurable velocity is indicated in Fig. 11.

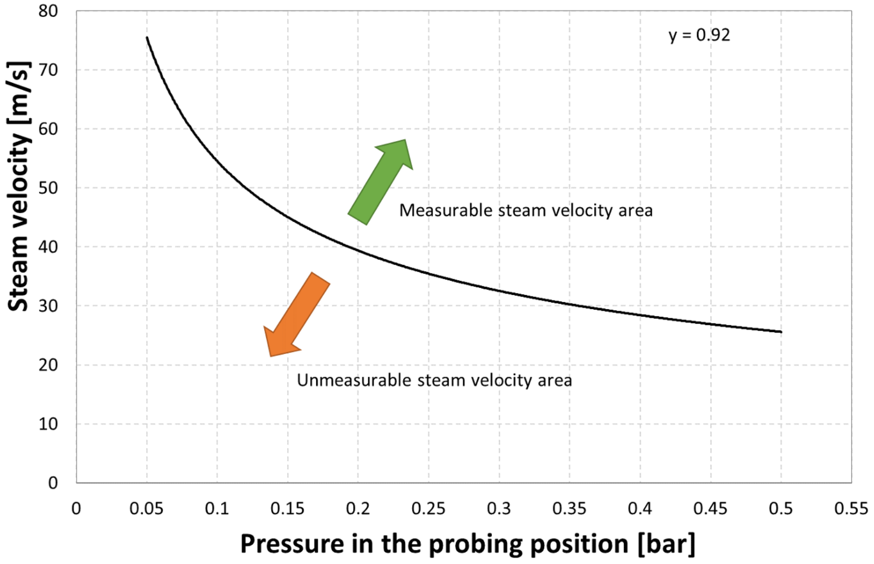

Fig. 11. Multi-hole probe measurable region.

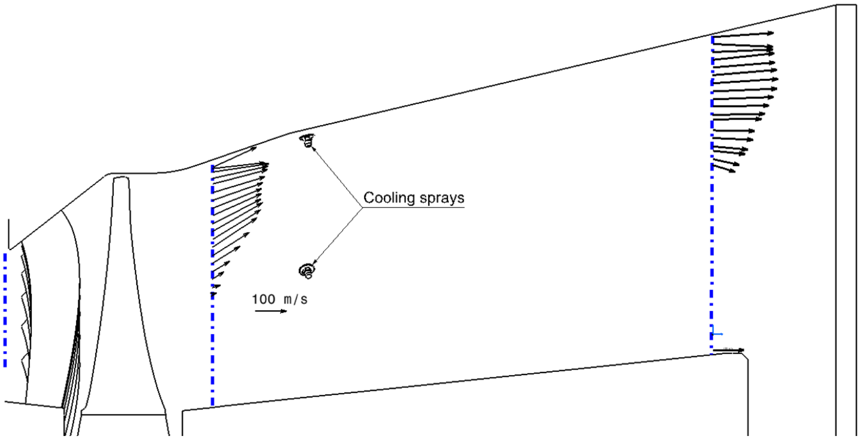

Fig. 12. Measured meridional velocities for low-load regime ($\varphi \cong 0.18$).

The velocity profiles obtained from probing for the low-load regime ($\varphi \cong 0.18$) are shown in Fig. 12. Probing in plane 0 was not possible at all due to time constraints. In plane 2, it is evident that the velocity is immeasurably low in the lower half of the measured cross-section. The flow field character did not change at the axial casing exit. Here, too, the steam flowed only through the upper half of the cross-section. The lower half was not filled with steam, or there was inconspicuous reverse flow. This, combined with poorly designed cooling nozzles, can direct droplets towards the trailing edges of the blades, causing their subsequent erosion [10].

The final type of results obtained is the relationship between the temperatures and pressures around the last rotor blade and the amplitude of blade vibrations, measured using blade tip-timing. The critical dependence is the pressure ratio $\pi \equiv p_{2t} / p_{1t} = f(\varphi)$ while incorporating the third dimension, which is the amplitude of blade tip vibrations. This relationship is depicted in Fig. 13. In the normal range of operating regimes, vibrations are close to zero. They increase if the blade is aerodynamically choked and a shock wave passes through the inter-blade channel. As the operating regime approaches low-load conditions, vibrations begin to increase when approaching the ventilation limit, particularly when $\pi > 0.9$. At $\varphi = 0.1$, the pressure ratio is maximized (1.15), and so are the vibration levels. This phenomenon occurred when the turbine was phased in to the power grid.

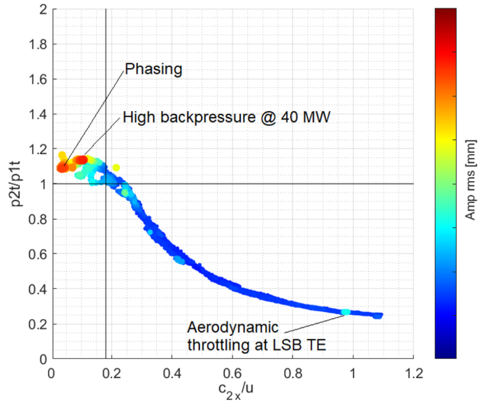

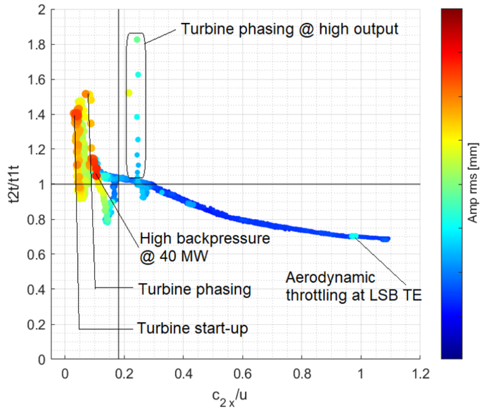

Fig. 13. Pressures around last stage bucket tip over the whole turbine operation spectra.

Fig. 14. Temperatures around last stage bucket tip over the whole turbine operation spectra.

With further reduction in the turbine's steam flow, the pressure ratio π decreased (the steam flow and hence c_{2x} were reduced), yet the pressure ratio remained higher than 1. When the turbine was phased in at minimal power, significant blade tip vibrations were also observed.

Similar characteristics are found in the temperature ratio profile across the blade tip τ, as shown in Fig. 14. Temperatures behind the rotor blade were up to 1.8 times higher than in front of it, which occurred when the turbine was phased in at higher power. Under normal operating conditions and during turbine start-up, temperatures behind the blade reached up to 1.5 times higher. Alongside the high amplitude of blade tip vibrations, there is evident extreme stress on the last rotor blade during low-load regimes.

4 Conclusions

Experiments were conducted on a 200 MW turbine to investigate steam flow behavior in the area of the last stage and the exhaust hood. Experimentally, pressure and temperature values were recorded on the turbine walls and their vicinity. Additionally, pneumatic probes were used to determine steam flow velocity profiles for nominal and ventilation regimes before and after the last stage, as well as at the diffuser outlet. Using the blade tip-timing method, amplitude values of blade tip vibrations were added to the flow data. The measured parameters were plotted depending on the ventilation coefficient c_{2x} / u.

It was experimentally demonstrated that compression in the exhaust hood depends on the turbine regime and its magnitude differs for the left and right sides of the machine. The greatest compression occurs just behind the trailing edges of the last stage blades. Compression decreases towards the outlet part of the casing.

By measuring the pressure before (p_0) and after (p_2) the last stage, a limiting pressure ratio can be identified, at which the flow direction reverses and steam is compressed through the blade tips. When the steam flow direction reverses, temperatures in the blade tip region also rise. The highest temperature in this area can easily reach up to 200°C.

The steam flow character was confirmed using a multi-hole probe. Under nominal regime, the flow was forward and uniform in all locations. Under low-load regime, the flow was forward in the upper half of the stage, but the velocity in the lower half was immeasurably low. There is reverse steam flow from the casing to the stage, and cooling the turbine end with water nozzles poses a risk of trailing edge erosion.

Under low-load regimes, the pressure behind the blade tip can be up to 15% higher, and the temperature up to 80% higher, than in front of the blade. Simultaneously, blade tip vibrations occur under these conditions. For turbine and blade design, it is essential to know and understand these limiting parameters. This contribution aims to serve that purpose.

Authors thank for the financial contribution to the Technology Agency of the Czech Republic, programme Théta 2, project number TS02020040.

References

1. B. Megerle, I. McBean, T. Stephen Rice, and P. Ott, (May 2, 2014). "Unsteady Aerodynamics of Low-Pressure Steam Turbines Operating Under Low Volume Flow." ASME. J. Turbomach. September 2014; 136(9): 091008. https://doi.org/10.1115/1.4027373
2. T. Tanuma, M. Ogawa, H. Okuda, G. Hashimoto, N. Shibukawa, K. Okuno, T. Tsukuda, "Unsteady Flow Effects on Steam Turbine Last Stage Blades at Very Low

Load Operating Condition." Proceedings of the ASME Turbo Expo 2018: Oslo, Norway. June 11–15, 2018. V008T29A028. ASME.
https://doi.org/10.1115/GT2018-76498

3. T. Tanuma, H. Okuda, T. Haraguchi, K. Okuno, N. Shibukawa, "A Study of Unsteady Aerodynamic Forces on Last Stage Blades in a Low-Pressure Model Steam Turbine at Very Low Operating Conditions." Proceedings of the ASME Turbo Expo 2023: Boston, Massachusetts, USA. June 26–30, 2023. V010T20A003. ASME. https://doi.org/10.1115/GT2023-101083
4. B.R. Haller, T.S. Rice, R. Sigg, "Alleviation of Rotating Pressure Oscillations in the Last LP Turbine Stage During Low-Load Conditions." Proceedings of the ASME Turbo Expo 2016. Seoul, South Korea. June 13–17, 2016. V008T26A004. ASME. https://doi.org/10.1115/GT2016-56088
5. A. Beevers, S. Havakechian, B. Megerle, (May 12, 2015). "On the Prediction and Theory of the Temperature Increase of Low Pressure Last Stage Moving Blades During Low Volume Flow Conditions, and Limiting it Through Steam Extraction Methods." ASME. J. Turbomach. October 2015; 137(10): 101002. https://doi.org/10.1115/1.4030258
6. E. Landrum, Z. Wu, A. Kulkarni, C. Musch, "Development of Multiphase Computational Fluid Dynamics Simulation for Predicting Last Stage Low Pressure Steam Turbine Blade Water Droplet Erosion." Proceedings of the ASME Turbo Expo 2023. Boston, Massachusetts, USA. June 26–30, 2023. V010T20A014. ASME. https://doi.org/10.1115/GT2023-103178
7. M. Xu, L. Cao, H. Luo, P. Hu, Y. Wang, "Effect of water spray in exhaust passage of steam turbine on flow field of the last stage during windage." International Journal of Heat and Mass Transfer, Volume 161, 2020, 120296, https://doi.org/10.1016/j.ijheatmasstransfer.2020.120296
8. M. Hoznedl, Z. Ruml, J. Vlasák, J. Bém, M. Ranš, "Cooling of Steam Turbine Exhaust Hood and Last Stage Blade." MATEC Web Conf., 383 (2023) 00010 https://doi.org/10.1051/matecconf/202338300010
9. H. Mistry, et al. "Aerodynamic Performance Assessment of Part-Span Connector of Last Stage Bucket of Low Pressure Steam Turbine." Proceedings of the ASME 2011 Power Conference, Volume 1. Denver, Colorado, USA. July 12–14, 2011. pp. 545-550. ASME.
https://doi.org/10.1115/POWER2011-55265
10. N. Sürken, A. Hofbauer, D. Pfaller, "Trailing Edge Erosion Prevention in Steam Turbine Last Stage Rotating Blades." Proceedings of the ASME Turbo Expo 2023: Volume 10, Boston, Massachusetts, USA. June 26–30, 2023. V010T20A026. ASME. https://doi.org/10.1115/GT2023-103990